Korean J. Chem. Eng., 33(8), 2460-2468 (2016)
DOI: 10.1007/s11814-016-0104-8

pISSN: 0256-1115
eISSN: 1975-7220

Density, viscosity, refraction index and excess properties of binary mixtures of 1-(1-methypiperidinium-1-yl) pentane-(1-pyridinium) bis(trifluoromethane) sulfonamide with acetonitrile at T=(293.15 to 323.15) K

Jun Wang†, Hao Song, Xuzhao Yang, Wenyuan Zou, Yufei Chen, Shaochan Duan, and Jun Sun

Henan Provincial Key Laboratory of Surface and Interface Science,
Collaborative Innovation Center of Environmental Pollution Control and Ecological Restoration,
Zhengzhou University of Light Industry, Zhengzhou 450002, P. R. China
(*Received 17 February 2016 • accepted 14 April 2016*)

Abstract−The density, viscosity, and refractive index of a pure asymmetrical dicationic ionic liquid, 1-(1-methypiperidinium-1-yl) pentane-(1-pyridinium) bis(trifluoromethane)sulfonamide, and its binary mixtures with acetonitrile were investigated at temperatures from 293.15 K to 323.15 K over the entire range of composition at ambient pressure. From the experimental data, the excess molar volumes, dynamic viscosity deviations, and refractive index deviations were, respectively,calculated and correlated with Redlich-Kister-type polynomials. The temperature dependence of viscosity for pure ionic liquid was described by modified Vogel-Tammann-Fulcher (VTF) equation. The enthalpy and entropy of activation for viscous flow were obtained. The values of molar refraction and polarizability indicated that the dominant interactions between ionic liquids and acetonitrile were dipole-dipole molecular interactions. These thermodynamic properties were discussed in terms of nature of molecular interactions between the ionic liquid and acetonitrile.

Keywords: Density, Viscosity, Refraction Index, Excess Properties, Ionic Liquid

INTRODUCTION

Ionic liquids (ILs) are specific kinds of organic salts obtained from a combination of organic cations and organic or inorganic anions. ILs have been applied successfully in electrochemistry, material chemistry, nanotechnology, polymer science, and organic synthesis [1-6].

The surge of interest in ILs is attributed to their unique properties, such as negligible vapor pressure, low melting points, suitable viscosity, high conductivity, wide electrochemical windows, and high stability. These properties allow the successful use of ILs as agents for developing clean technologies [7-10].

Dicationic ILs (DILs) are a novel type of ILs composed of anions and doubly charged cations that consist of two singly charged cations with linkage. The variation of cations and linkage has given IL its amount and diversity such that it possesses a wider liquid range and higher thermal stability compared with traditional monocationic ILs. Therefore, DILs can be designed based on the required properties; these materials are more suitable for lubrication [11,12], chromatography [13,14], and catalysis [15-17]. Research on the physical properties of DILs is required for future applications in the industry. To date, experimental data of physicochemical properties of DILs are unfortunately still limited. The density, viscosity, and refractive index of pure DILs and their mixtures with organic solvents are known to be important properties in multiple processes that involve heat and mass transfer. Density and viscosity are the key properties for process design and equipment options as a result of their effect on mixing, separation, and transportation [18,19]. The refractive index (n_D) can be used to determine the electronic polarizability of a molecule and provides information on the intermolecular force [20]. In addition, knowledge of these properties is meaningful and helpful to the development of theoretical simulations, which are powerful tools for predicting the behavior of these pure DILs and their mixtures [21,22].

In this work, we synthesized and characterized a novel asymmetrical DIL, 1-(1-methypiperidinium-1-yl) pentane-(1-pyridinium) bis(trifluoromethane)sulfonamide ($[PiC_5Py][NTf_2]_2$, Scheme 1). The experimental densities, viscosities, and refractive indexes of $[PiC_5Py][NTf_2]_2$ and its binary mixtures with acetonitrile (ACN) were determined over the entire composition range at temperatures (T) from 293.15 K to 323.15 K under atmospheric pressure. The dependence on temperature of the viscosity of $[PiC_5Py][NTf_2]_2$ was fitted to the modified VFT equation. The density deviations, excess molar volumes (V^E), viscosity deviations ($\Delta\eta$), and refractive deviations (Δn_D) of the binary mixtures were calculated and fitted with Redlich-Kister-type polynomials. To investigate the intermolecular

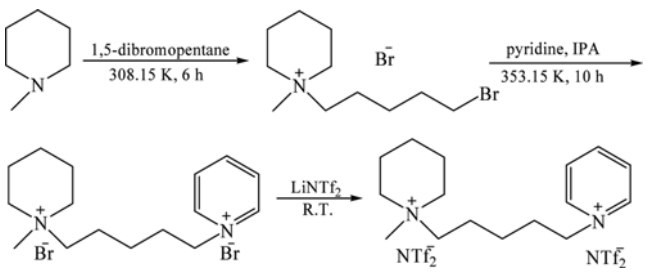

Scheme 1. Synthetic process of $[PiC_5Py][NTf_2]_2$.

†To whom correspondence should be addressed.
E-mail: wangjun8828@sina.com

interactions between DIL and solvents, the values V^E, molar refraction, and polarizability, as well as the excess Gibbs energy (ΔG^{*E}), enthalpy (ΔH^*), and entropy (ΔS^*) of activation for viscous flow, were all obtained and discussed in the present work. To the best of our knowledge, this study is the first to focus on these thermodynamic properties of DILs.

EXPERIMENTAL

1. Materials and Preparation of Solutions

The studied IL $[PiC_5Py][NTf_2]_2$ was synthesized with a mass fraction purity>0.995. 1-Methylpiperidine ($C_6H_{13}N$, CAS. 626-67-5), pyridine (C_5H_5N, CAS. 110-86-1), and 1,5-dibromopentane ($C_5H_{10}Br_2$, CAS. 111-24-0) were purchased from Aladdin Industrial Inc. Bis(trifluoromethane)sulfonimide lithium salt ($C_2F_6LiNO_4S_2$, CAS. 90076-65-6) was obtained from the Lanzhou Institute of Chemical Physics, whereas ACN (C_2H_3N, CAS. 75-05-8) and ethyl acetate ($C_4H_8O_2$, CAS. 141-78-6) were obtained from the Tianjin Kermel Chemical Reagent Co., Ltd. All chemicals were used without further purification. The sources and mass fraction purity of the materials are given in Table 1. The density, viscosity, and refractive index of ACN are determined and compared with the literature in Table 2.

Solutions were gravimetrically prepared with an analytical balance that has an accuracy of $\pm 1\times10^{-4}$ g in the mass fraction. The mixtures were degassed in an ultrasonic bath to eliminate air in the solutions. No decomposition of IL was observed at the experimental conditions.

2. Synthesis and Characterization of Dicationic IL

$[PiC_5Py][NTf_2]_2$ was synthesized according to the following procedure: 1-Methylpiperidine (31.1 g, 0.31 mol) was added dropwise to 1,5-dibromopentane (427.7 g, 1.86 mol) in 20 h at 308.15 K. The mixture was stirred for 15 h. The resulting residue was washed thrice (3×200 ml) with ethyl acetate to remove any unreacted reactants, followed by filtration to produce a white precipitate, which was dried under vacuum. The solid precipitate (93.9 g, 0.286 mol) was dissolved in isopropanol (100 ml) before pyridine (27.1 g, 0.343 mol) was added, and the solution was stirred at 353.15 K for 20 h. The solvent was removed by distillation and residue was extracted thrice (3×200 ml) with ethyl acetate. After filtration, the solvent was removed under vacuum at 333.15 K for 24 h, to produce the white 1-(1-methypiperidinium-1-yl) pentane-(1-pyridinium) dibromide powder. 1-(1-Methypiperidinium-1-yl) pentane-(1-pyridinium) dibromide (114.0 g, 0.27 mol) was added to 300 mL of water, whereas bis(trifluoromethane)sulfonimide lithium salt (155.0 g, 0.54 mol) was added to 200 mL water. Both solutions were mixed, and the mixture was stirred for 10 h at room temperature. The water was removed, and the resulting residue was washed with water until no bromide ions were detected. The yield was 85.3%. The water content of the final IL was analyzed by Karl-Fisher titration. The mass fraction of water in the IL is 0.001%. The DIL was analyzed by ^{1}H NMR and IR to confirm the constitution and absence of any major impurities. ($[PiC_5Py][NTf_2]_2$ ^{1}H NMR (400 MHz, $CDCl_2$)

Table 1. Specification of used materials

Chemical	CAS number	Purity/in mass fraction	Source
1-Methylpiperidine	626-67-5	>0.970	Aladdin Industrial Inc., China
Pyridine	110-86-1	>0.990	Aladdin Industrial Inc., China
1,5-Dibromopentane	111-24-0	>0.990	Yancheng Longsheng Chemical Co., Ltd., China
Lithium bis(trifluoromethane)sulfonimide	90076-65-6	>0.990	Lanzhou Institute of Chemical Physics, China
Acetonitrile	75-05-8	>0.995	Tianjin Kermel Chemical Reagent Co., Ltd., China
Ethyl acetate	141-78-6	>0.995	Tianjin Kermel Chemical Reagent Co., Ltd., China

Table 2. Comparison of experimental density, viscosity, and refractive index values of pure acetonitrile with literature values at different temperature

Properties	T/K	Exp.	Lit.
ρ/(g·cm^{-3})	293.15	0.7812	0.78189 [26], 0.782005 [23], 0.7820 [27]
	303.15	0.7715	0.77112 [26], 0.771487 [24], 0.7713 [25]
	313.15	0.7608	0.76020 [26], 0.760541 [24], 0.7603 [27]
	323.15	0.7496	0.749449 [24], 0.7494 [25], 0.7492 [27]
η/(mPa·s)	293.15	0.3595	0.355 [23], 0.3645 [27], 0.364 [24]
	303.15	0.3214	0.329 [34], 0.332 [25], 0.3307 [27]
	313.15	0.2904	0.300 [34], 0.304 [25], 0.3005 [27]
	323.15	0.2635	0.276 [34], 0.279 [25], 0.2746 [27]
n_D	293.15	1.3429	1.3439 [23], 1.3409 [29]
	303.15	1.3394	1.3395 [28], 1.3392 [29]
	313.15	1.3348	1.3347 [28], 1.3260 [29]
	323.15	1.3297	

The standard uncertainties u are u(ρ)=±0.00005 g·cm^{-3}, u(T)=±0.03 K, u(η)=0.0001 mPa·s, and u(n_D)=0.0001, u(p)=5 kPa

d (ppm): 1.53 δ (m, 2H, 11-CH_2), 1.70 δ (m, 2H, 15-CH_2), 1.77 δ (m, 2H, 13-CH_2), 1.97 δ (m, 4H, 12, 14-CH_2), 2.50 δ (m, 2H, 10-CH_2), 2.98 δ (m, 3H, 16-CH_3), 3.30 δ (m, 6H, 7, 8, 9-CH_2), 4.62 δ (t, 2H, 6-CH_2), 8.20 δ (t, 2H, 1, 5-H), 8.62 δ (t, 1H, 3-H), 9.08 δ

Table 3. Experimental data for binary system of $[PiC_5Py][NTf_2]_2$ (1) and acetonitrile (2) at atmospheric pressure

x_1	ρ/(g·cm^{-3})	V^E/(cm^3·mol^{-1})	η/(mPa·s)	$\Delta\eta$/(mPa·s)	n_D	Δn_D
			293.15 K			
0.0000	0.7812	0.0000	0.3595	0.0000	1.3429	0.0000
0.1000	1.1965	−1.5639	3.5448	−204.7781	1.4067	0.0530
0.1998	1.3345	−1.7304	15.6346	−400.2358	1.4255	0.0609
0.2966	1.4020	−1.7016	48.1335	−569.0455	1.4389	0.0638
0.3883	1.4405	−1.5126	121.7014	−686.1800	1.4397	0.0547
0.4939	1.4694	−1.1218	282.4011	−745.0897	1.4448	0.0483
0.5956	1.4895	−0.8515	517.5690	−721.4206	1.4468	0.0393
0.6954	1.5048	−0.7414	780.1862	−666.3509	1.4485	0.0301
0.7906	1.5153	−0.3417	1050.0539	−594.4643	1.4494	0.0207
0.8879	1.5243	−0.0947	1477.0002	−369.8664	1.4506	0.0114
1.0000	1.5334	0.0000	2079.9936	0.0000	1.4514	0.0000
			303.15 K			
0.0000	0.7715	0.0000	0.3214	0.0000	1.3394	0.0000
0.1000	1.1871	−1.6566	2.73133	−91.34438	1.4047	0.0543
0.1998	1.32606	−1.88547	10.9700	−176.6726	1.4233	0.0619
0.2966	1.3933	−1.7990	30.4152	−247.9815	1.4364	0.0643
0.3883	1.4323	−1.6322	71.6812	−292.6882	1.4379	0.0557
0.4939	1.4615	−1.2675	155.3008	−308.0732	1.4423	0.0485
0.5956	1.4821	−1.0965	271.3310	−287.3911	1.4455	0.0405
0.6954	1.4975	−0.9941	389.5941	−262.6948	1.4456	0.0296
0.7906	1.5081	−0.6483	503.9174	−237.6255	1.4473	0.0208
0.8879	1.5171	−0.3625	681.9501	−150.8158	1.4487	0.0115
1.0000	1.5254	0.0000	937.8645	0.0000	1.4496	0.0000
			313.15 K			
0.0000	0.7608	0.0000	0.2904	0.0000	1.3348	0.0000
0.1000	1.1765	−1.7210	2.1745	−44.8398	1.4024	0.0564
0.1998	1.3160	−1.9348	8.0250	−85.6198	1.4215	0.0643
0.2966	1.3840	−1.8809	20.3956	−118.4779	1.4340	0.0659
0.3883	1.4233	−1.7150	44.8248	−136.8945	1.4364	0.0580
0.4939	1.4539	−1.5532	92.1359	−138.9239	1.4398	0.0496
0.5956	1.4740	−1.2450	154.1206	−124.4575	1.4421	0.0405
0.6954	1.4894	−1.1324	212.7511	−112.4575	1.4429	0.0301
0.7906	1.5002	−0.05320	266.0690	−103.6208	1.4450	0.0215
0.8879	1.5092	−0.1814	347.5582	−67.5939	1.4466	0.0122
1.0000	1.5172	0.0000	467.5296	0.0000	1.4470	0.0000
			323.15 K			
0.0000	0.7496	0.0000	0.2635	0.0000	1.3297	0.0000
0.1000	1.1663	−1.8567	1.7942	−25.4964	1.4008	0.0596
0.1998	1.3070	−2.1234	6.15334	−48.1104	1.4209	0.0682
0.2966	1.3757	−2.1018	14.4738	−65.9523	1.4326	0.0687
0.3883	1.4154	−1.9561	30.3703	−74.8397	1.4344	0.0600
0.4939	1.4458	−1.7160	59.7928	−73.9579	1.4379	0.0513
0.5956	1.4669	−1.6128	97.1427	−64.0947	1.4405	0.0422
0.6954	1.4822	−1.4328	130.0572	−58.1532	1.4416	0.0318
0.7906	1.4935	−1.2366	159.8632	−54.0772	1.4436	0.0228
0.8879	1.5023	−0.8561	204.9049	−35.3329	1.4445	0.0125
1.0000	1.5093	0.0000	270.5352	0.0000	1.4449	0.0000

Standard uncertainties (u) are u(x_1)=0.0001, u(ρ)=±0.00005 g·cm^{-3}, u(T)=±0.03 K, u(η)=0.0001 mPa·s, and u(n_D)=0.0001, u(p)=5 kPa

(m, 2H, 1, 5-H). IR (KBr): 3,145 cm^{-1}, 3,110 cm^{-1}, 2,949 cm^{-1}, 2,882 cm^{-1}, 1,638 cm^{-1}, 1,490 cm^{-1}, 822 cm^{-1}, 779 cm^{-1}, 692 cm^{-1}, and 561 cm^{-1}).

3. Apparatus and Experimental Procedure

3-1. U-tube Density Measurements

The density (ρ) data of pure DIL and its binary mixtures were measured with a Rudolph DDM 2911 vibrating U-tube densitometer in the T range from 303.15 K to 323.15 K. The accuracy and precision of the densitometer were ±0.00005 g·cm^{-3}. The temperature of the measure cell was automatically set within ±0.03 K. The apparatus was calibrated with clean dry ambient air, ultrapure water, and tetrachloroethylene at atmospheric pressure before each series of measurements. Each experimental density value is the average of three measurements at one temperature. The relative uncertainty of the density measurements was estimated to be ±0.05%. The experimental values of ACN are compared with those in literature [23-27] in Table 2.

3-2. Capillary Viscosity Measurements

The viscosity was measured with a suspended level micro-Ubbelohde capillary viscometer of different diameters, which was immersed in the water thermostat at different temperatures. Before measurement, each capillary viscometer was calibrated with ultrapure water and viscosity standard oil purchased from the Cannon Instrument Company. The flow time of the constant volume of liquid through a capillary was measured with an electronic stopwatch; the average of six reading did not exceeded ±0.02 s for each solution. The relative uncertainty of the viscosity measurements was estimated to be ±1.0%. A comparison of the measured viscosity values of ACN with those published in literature [23-25,27] at the experimental temperatures is listed in Table 2. The measurement results showed considerable consistency.

3-3. Refractive Index Measurements

Refractive indexes were determined under natural light with a manual refractometer. The apparatus is provided with thermostatic prisms, which are connected to a water thermostat controlled within ±0.01 K. The apparatus was calibrated with ultrapure water and 1-bromonaphthalene. The standard uncertainty in the instrument of the refractive index was estimated to be 0.01%. The comparison of measured values of ACN with those published in literature [23,28, 29] is presented in Table 2.

RESULTS AND DISCUSSION

1. Densities and Volumetric Properties of $[PiC_5Py][NTf_2]_2$ (1)+ ACN (2) Mixtures

The experimental values of density, ρ, for the binary mixture system of $[PiC_5Py][NTf_2]_2$+ACN at different temperatures over the entire composition range are presented in Table 3. A linear relation can be observed for the temperature dependence of the system at all mole fractions.

The extent of deviation of mixtures from ideal behavior was well expressed by V^E, which was determined from the measured densities with the following equation:

$$V^E = \frac{[x_1M_1+(1-x_1)M_2]}{\rho} - \frac{x_1M_1}{\rho_1} - \frac{(1-x_1)M_2}{\rho_2} \quad (1)$$

where x_1 is mole fractions of $[PiC_5Py][NTf_2]_2$, $(1-x_1)$ is mole fractions of ACN. ρ_1, ρ_2, and ρ are the densities of $[PiC_5Py][NTf_2]_2$, ACN, and their mixture, respectively. M_1 and M_2 are the molar mass of $[PiC_5Py][NTf_2]_2$ and ACN.

The experimental values of V^E have been fitted with Redlich-Kister-type polynomials:

$$V^E = x_1(1-x_1)\sum_i A_i(2x_1-1)^i \quad (2)$$

where x_1 is the mole fraction of $[PiC_5Py][NTf_2]_2$, and A_i are the Redlich-Kister parameters obtained by fitting the experimental values with a least-squares-type algorithm. The standard deviation (σ) as defined in the following equation is given for each value in Table 4.

$$\sigma = \left[\sum \frac{(V^E_{exp} - V^E_{cal})^2}{n}\right]^{1/2} \quad (3)$$

Table 4. Parameters of Redlich-Kister-type polynomial and standard deviation (σ) for the binary mixture

T/K	A_0	A_1	A_2	A_3	σ
			V^E/(cm^3·mol^{-1})		
293.15	−4.54521	4.82249	−6.32161	8.07023	0.058718
303.15	−5.16627	3.85973	−8.37871	8.09278	0.047059
313.15	−5.84163	3.35944	−8.33084	8.26898	0.056934
323.15	−6.77579	2.72975	−11.0886	6.83837	0.052518
			$\Delta\eta$/(mPa·s)		
293.15	−2952.26	−403.875	−167.257	−1032.89	11.03504
303.15	−1213.67	20.9324	−121.235	−649.659	5.270962
313.15	−544.519	103.730	−87.3039	−408.234	2.730471
323.15	−289.318	89.2725	−60.0711	−252.268	1.673977
			Δn_D		
293.15	0.18552	−0.15343	0.22151	−0.21088	0.001673
303.15	0.18739	−0.15583	0.22586	−0.22026	0.001795
313.15	0.19100	−0.16764	0.24270	−0.21381	0.001802
323.15	0.19791	−0.16927	0.26506	−0.24478	0.001676

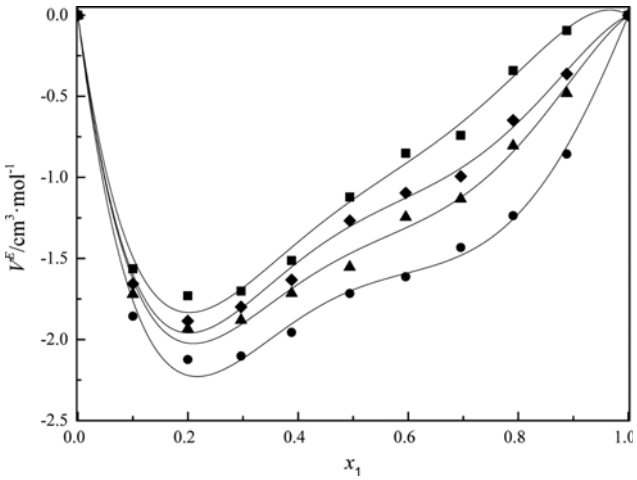

Fig. 1. Excess molar volumes with mole fraction of the binary system at different temperatures: ■, 293.15 K; ◆, 303.15 K; ▲, 313.15 K; ●, 323.15 K. The solid curves represent the values calculated with Eq. (2).

where V^E_{exp} are the experimental value and V^E_{cal} are the calculated value from Eq. (2), n is the number of experimental data.

The V^E for the binary mixture are negative over the entire composition range at all surveyed temperatures (Fig. 1). The minimal values of V^E were observed at approximately x_1=0.2. The values of V^E of a mixture that contains polar compounds are the result of a number of effects, which may contribute in terms of changing the sign. The disruption of self-association in the $[PiC_5Py][NTf_2]_2$ or ACN has a positive contribution to V^E, but the specific interaction between $[PiC_5Py][NTf_2]_2$ and ACN has a negative contribution. The free volume effect depends on differences in the characteristic pressures and temperatures of the components, and has a negative contribution. Meanwhile, the interstitial accommodation and the effect of the condensation of $[PiC_5Py][NTf_2]_2$ with ACN provide additional negative contributions to V^E.

The excess volume of the binary mixture has a negative deviation over the entire mole fraction range (Fig. 1), thereby indicating that the free volume effect of different temperatures of the components, the packing efficiency of ACN accommodation in the interstitial regions of $[PiC_5Py][NTf_2]_2$ networks, and the interaction of ion-dipole and hydrogen bonding dominate in the binary mixture [30]. According to literature [30,31], the absolute value of V^E of the binary mixture indicates the difference in the packing efficiency and the interaction intensity. The V^E values for the $[PiC_5Py][NTf_2]_2$+ACN system are more negative than in the [BMPyr][NTf_2]+ACN [32] and [BMIm][NTf_2]+ACN [33] systems, thereby suggesting a strong interaction between $[PiC_5Py][NTf_2]_2$ and ACN. Even if the molecular volume of $[PiC_5Py][NTf_2]_2$ lowers the packing efficiency, which leads to a small $|V^E|$ value, the high polarity of $[PiC_5Py][NTf_2]_2$ enhances the interaction between cations of $[PiC_5Py][NTf_2]_2$ and ACN. The strong ion-dipole interaction between the non-hydrogen bonding polar solvents and cations of $[PiC_5Py][NTf_2]_2$ leads to the large $|V^E|$ value [34].

The influence of temperature on V^E is also discussed, the variation of V^E values (Table 3) is caused by the competition of the hydrogen bonding interaction and packing efficiency in the mixture. The increasing temperature generally reduces the hydrogen bonding, thereby increasing the V^E values, and strengthens the packing efficiency, thereby decreasing the V^E values [35]. For the $[PiC_5Py][NTf_2]_2$+ACN binary mixture, the reduced hydrogen bonding has an energetic role in the transformation of V^E values.

2. Viscosities and Thermodynamic Properties of $[PiC_5Py][NTf_2]_2$ (1)+Acetonitrile (2) Mixtures

The dynamic viscosities (η) for the binary mixtures of $[PiC_5Py][NTf_2]_2$ (1)+ACN (2) at different temperatures over the entire composition range were determined and presented in Table 3. The viscosity of pure $[PiC_5Py][NTf_2]_2$ can be expressed as a function of temperature over the entire composition range. A modification of the Vogel-Tammann-Fulcher (VTF) equation can be expressed as [36]:

$$\eta = AT^{0.5}e^{[-B/(T-T_0)]} \quad (4)$$

where the adjustable parameters are A (mPa·s), B (K) and the glass-transition temperature, T_0 (K).

The calculated values of the adjustable parameters for viscosity of pure $[PiC_5Py][NTf_2]_2$, ACN and their mixtures are listed in Table 5. In addition, the correlation square coefficient and the standard relative deviations are given. In accordance with the results, the modified VFT equation is available method to fit the viscosity data.

According to the experimental values for the viscosity of the binary

Table 5. Parameters of modified VFT equation and the standard relative deviations (σ) for the binary mixture

x_1	$A\times10^3$	$B\times10^{-3}$	$T_0\times10^{-2}$	R^2	σ
0.0000	0.52650	−1.02492	0.15069	0.99998	0.00017
0.1000	4.31104	−0.49921	1.64217	0.99998	0.00271
0.1998	3.94336	−0.74136	1.56998	0.99999	0.01410
0.2966	3.44870	−0.87582	1.62499	0.99999	0.02364
0.3883	2.95168	−1.02716	1.61241	0.99997	0.19676
0.4939	4.77855	−0.99446	1.71082	0.99998	0.37452
0.5956	5.12933	−1.04618	1.72647	0.99997	0.86874
0.6954	6.13421	−1.02848	1.78097	0.99997	1.48821
0.7906	6.02704	−1.03704	1.80769	0.99996	2.03930
0.8879	5.94950	−1.06174	1.82345	0.99995	3.36726
1.0000	5.37242	−1.13049	1.80399	0.99996	4.64551

mixtures of $[PiC_5Py][NTf_2]_2$ and ACN, $\Delta\eta$ was calculated with the following equation:

$$\Delta\eta=\eta-(x_1\eta_1+x_2\eta_2) \quad (5)$$

where η, η_1 and η_2 are the absolute viscosity of the binary mixtures, $[PiC_5Py][NTf_2]_2$ and ACN; x_1 is mole fractions of $[PiC_5Py][NTf_2]_2$, x_2 is mole fractions of ACN. The values of $\Delta\eta$ are given in Table 3. The values of $\Delta\eta$ were fitted with the Redlich-Kister-type polynomial at different temperatures, and parameters are listed in Table 4.

The values of $\Delta\eta$ are negative from each curve of the binary mixture at all composition ranges (Fig. 2); the minimum value was observed at approximately x=0.5. In accordance with literature [30, 37], $\Delta\eta$ of a mixture reflects the competition between the molecular interaction and size. When the mixture is dominated by intermolecular forces, the values of $\Delta\eta$ are negative. By contrast, values of $\Delta\eta$ are positive when the mixture is dominated by hydrogen bonds between $[PiC_5Py][NTf_2]_2$ and ACN. According to the values of $\Delta\eta$ for the binary mixture in Fig. 2, the negative deviations may be attributed to the strong self-association of ACN and the weak hydrogen bonding interaction between $[PiC_5Py][NTf_2]_2$ and ACN. As the temperature increases, the values of $\Delta\eta$ become less negative and more flat, and the absolute values decrease. The temperature strongly influences $\Delta\eta$ but the observed compositions at the maximum $\Delta\eta$ were almost constant and independent of temperature.

On the basis of the theory of the absolute reaction rate, the ΔG^{*E} values were calculated with the following equation [38]:

$$\Delta G^{*E}=RT[\ln(\eta V)-x_1\ln(\eta_1V_1)-x_2\ln(\eta_2V_2)] \quad (6)$$

where R is the ideal gas constant, T is the absolute temperature, and V, V_1 and V_2 are the molar volumes of the binary mixtures, $[PiC_5Py][NTf_2]_2$ and ACN. The values of ΔG^{*E} are given in Table 6 and plotted in Fig. 4. As shown, the ΔG^{*E} for binary mixtures are positive over

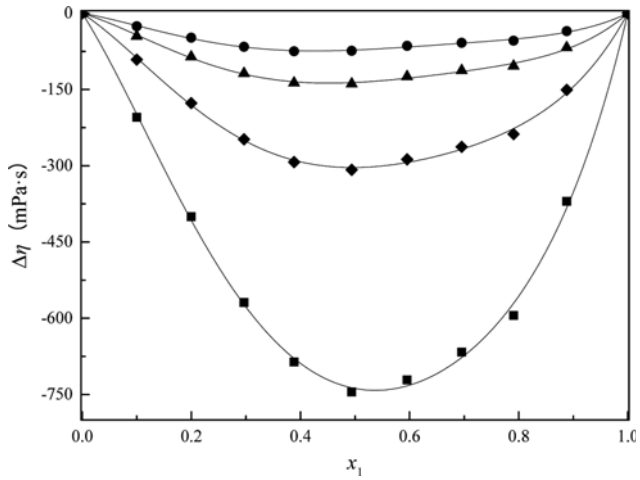

Fig. 2. Viscosity deviation with mole fraction of the binary system at different temperatures: ■, 293.15 K; ◆, 303.15 K; ▲, 313.15 K; ●, 323.15 K. The solid curves represent the values calculated with Eq. (2).

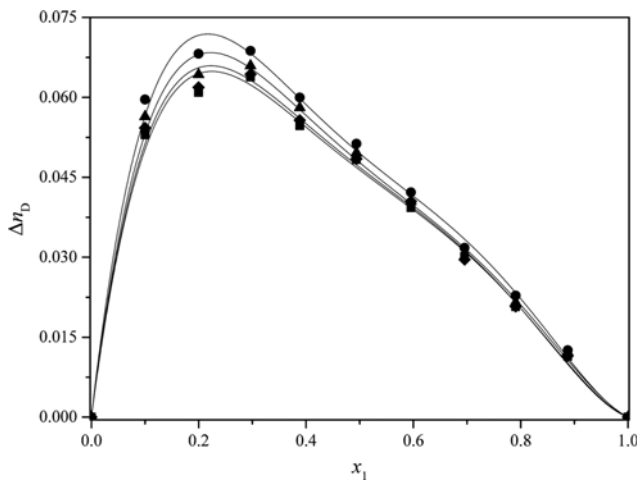

Fig. 3. Refractive index deviation with mole fraction of the binary system at different temperatures: ■, 293.15 K; ◆, 303.15 K; ▲, 313.15 K; ●, 323.15 K. The solid curves represent the values calculated with Eq. (2).

Table 6. Excess Gibbs free energy of activation for viscous flow (ΔG^{*E}) of the binary mixtures

x_1	ΔG^{*E}/(kJ·mol^{-1})			
	293.15 K	303.15 K	313.15 K	323.15 K
0.0000	0.0000	0.0000	0.0000	0.0000
0.1000	4.4351	4.3743	4.3336	4.3233
0.1998	6.3387	6.2770	6.2319	6.2035
0.2966	7.1602	7.0309	6.9337	6.8371
0.3883	7.4702	7.3331	7.2069	7.1067
0.4939	7.1725	7.0356	6.9257	6.8715
0.5956	6.3123	6.2017	6.1114	6.0358
0.6954	4.9679	4.8627	4.7821	4.7054
0.7906	3.4215	3.3289	3.2592	3.2038
0.8879	1.9029	1.8309	1.7725	1.7391
1.0000	0.0000	0.0000	0.0000	0.0000

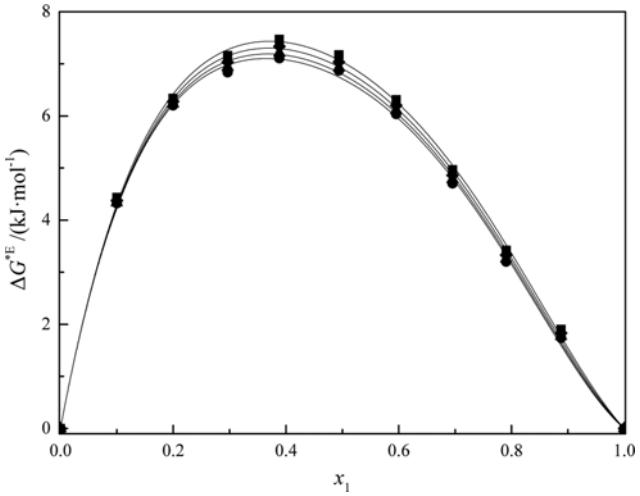

Fig. 4. Excess Gibbs free energies of activation for viscous flow with mole fraction of the binary system at different temperatures: ■, 293.15 K; ◆, 303.15 K; ▲, 313.15 K; ●, 323.15 K. The solid curves represent the values calculated with Eq. (2).

the entire composition range. The sign of the ΔG^{*E} values can be considered a reliable criterion for detecting or excluding the presence of interaction between different molecules, thereby indicating the formation of intermolecular hydrogen bonds between $[PiC_5Py][NTf_2]_2$ and ACN [35].

The activation thermodynamics, namely, ΔH^*, and ΔS^*, were evaluated based on Eyring's absolute reaction rate theory [39,40] with the viscosity expressed as

$$\eta = \frac{\rho h N_A}{M} \exp\left(\frac{\Delta G^*}{RT}\right) \quad (7)$$

where M is the average molar mass of the binary mixture, h is Planck's constant, N_A is Avogadro number, R is the ideal gas constant, and T is the absolute temperature. The values of Gibbs free energy of activation for the viscous flow (ΔG^*) are given in Table 7.

The values of ΔH^* and ΔS^* can be calculated with the equation:

$$R\ln\left(\frac{\eta M}{\rho h N_A}\right) = \frac{\Delta H^*}{T} - \Delta S^* \quad (8)$$

The terms on the left side of the equation were plotted against 1/T for each binary mixture. The ΔH^* and ΔS^* values were calculated from the slopes and intercepts and listed in Table 8. Above approximately x_1=0.2, the values of ΔH^* were higher than the $T\Delta S^*$ values. Therefore, the energetic contribution that corresponds to the molar ΔH^* is more important than the entropic contribution to the molar ΔG^*. Given the significant degree of hydrogen bonding, the self-association in the pure state and the strong cross association in their mixtures were observed [41]. The ΔS^* from the initial state to the transition state at a given composition is small during the activated viscous flow process. Generally, the increasing ΔS^* data showed that the viscous flow is an ordered process that involves contiguous liquid layers because of their self-association via hydrogen bonds and the existence of strong cross association in the corresponding binary mixtures. Consequently, their structural configuration is retained and even moves in a stationary steady state [42].

Table 7. Gibbs free energy of activation for viscous flow (ΔG^*) of the binary mixtures

x_1	$\Delta G^*/(kJ\cdot mol^{-1})$			
	293.15 K	303.15 K	313.15 K	323.15 K
0.0000	43.0757	44.2944	45.5273	46.7601
0.1000	50.1844	51.2591	52.3798	53.5592
0.1998	54.7564	55.7471	56.7920	57.9104
0.2966	58.1659	59.0087	59.9321	60.9406
0.3883	60.9277	61.6864	62.5152	63.4806
0.4939	63.4534	64.1244	64.8939	65.8195
0.5956	65.3123	65.9250	66.6414	67.5422
0.6954	66.6362	67.1713	67.8260	68.6827
0.7906	67.6352	68.1037	68.7010	69.5382
0.8879	68.7181	69.1263	69.6653	70.4825
1.0000	69.8123	70.1993	70.7165	71.5189

Table 8. Enthalpy of activation (ΔH^*) and entropy of activation (ΔS^*) for the viscous flow of the binary mixtures

x_1	$\Delta H^*/(kJ\cdot mol^{-1})$	$\Delta S^*/(J\cdot K^{-1}\cdot mol^{-1})$	R^2
0.0000	7.0600	−122.8438	0.9997
0.1000	17.2356	−112.3154	0.9974
0.1998	23.9751	−104.9047	0.9980
0.2966	31.0819	−92.2597	0.9980
0.3883	36.0809	−84.6066	0.9977
0.4939	40.4292	−78.3499	0.9972
0.5956	43.6478	−73.6894	0.9969
0.6954	46.7160	−67.9209	0.9963
0.7906	49.2079	−62.5882	0.9960
0.8879	51.6881	−57.7959	0.9955
1.0000	53.3571	−55.8317	0.9957

3. Refractive Indexes, Refractive Index Deviations, and Polarizability of $[PiC_5Py][NTf_2]_2$ (1)+ACN (2) Mixtures

The experimental values of n_D for the binary mixture of $[PiC_5Py][NTf_2]_2$ and ACN at different temperatures over the entire composition range are presented in Table 3. From the experimental values of n_D, the refractive index deviations (Δn_D) were calculated with the following equation:

$$\Delta n_D = n_D - x_1 n_{D1} - x_2 n_{D2} \quad (9)$$

where n_{D1}, n_{D2} are the refractive indexes of $[PiC_5Py][NTf_2]_2$ and ACN, respectively; and n_D is the refractive index of the binary mixture. Therefore, the values of Δn_D were obtained and included in Table 3 and Fig. 3. The composition dependence of the Δn_D of $[PiC_5Py][NTf_2]_2$ and ACN binary mixtures at different temperatures was fitted by Redlich-Kister-type polynomials. The parameters are given in Table 4.

The molar refraction (R_m) is calculated from the Lorentz-Lorenz equation [43]:

$$R_m = \left[\frac{n_D^2 - 1}{n_D^2 + 2}\right] V_m \quad (10)$$

where V_m is molar volume and n_D is the refractive index of the binary mixture. The values of molar refraction increase with the

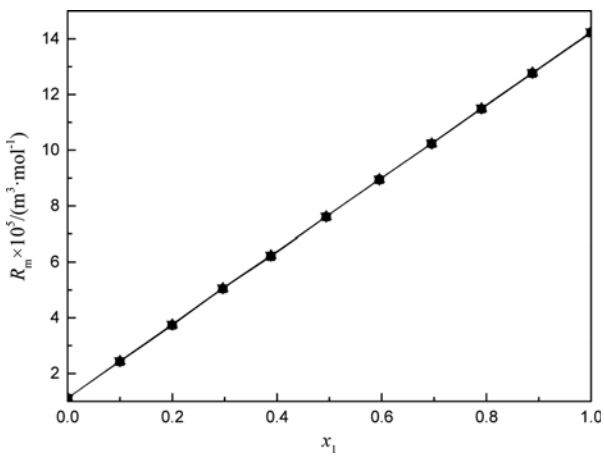

Fig. 5. Molar refraction with mole fraction of the binary system at different temperatures: ■, 293.15 K; ◆, 303.15 K; ▲, 313.15 K; ●, 323.15 K. The solid curves represent smoothed experimental data.

increasing composition of $[PiC_5Py][NTf_2]_2$ (Fig. 5). The value of molar refraction is directly proportional to the molecular polarizability, which is related to the ability of a molecular orbital to be impaired under an electrical field [44]. The electric dipole moment of the molecules absolutely dominated the orientation. The value of n_D is measured in the optical region; thus, the polarizability should not include the orientational effects [45]. Therefore, the molar refraction should not be regarded as a measure of the capacity molecular polarizability.

The significance of polarizability (α) is that it determines how the molecular electron cloud behaves under the effect of an electric field. This property is highly relevant for ILs due to the low electrostatic interactions which provide them their surprising and desirable characteristics [46]. The polarizability can be calculated by the following equation [47]:

$$\alpha=\left[\frac{n_D^2-1}{n_D^2+2}\right]\left[\frac{3V_m}{4\pi N_A}\right] \tag{11}$$

Table 9. Polarizability of the binary mixtures

x_1	$\alpha\times10^{29}/m^3$			
	293.15 K	303.15 K	313.15 K	323.15 K
0.0000	0.4400	0.4414	0.4422	0.4426
0.1000	0.9603	0.9637	0.9675	0.9725
0.1998	1.4783	1.4801	1.4868	1.4951
0.2966	1.9983	2.0007	2.0045	2.0109
0.3883	2.4581	2.4635	2.4716	2.4755
0.4939	3.0158	3.0174	3.0183	3.0239
0.5956	3.5417	3.5504	3.5464	3.5522
0.6954	4.0580	4.0550	4.0555	4.0649
0.7906	4.5503	4.5533	4.5568	4.5648
0.8879	5.0562	5.0618	5.0678	5.0702
1.0000	5.6336	5.6436	5.6456	5.6520

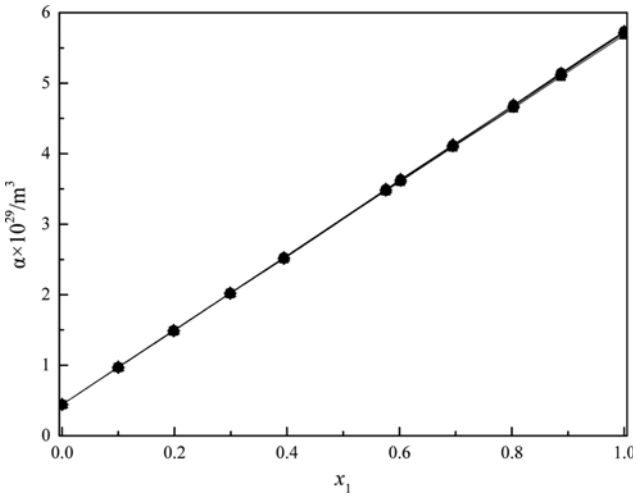

Fig. 6. Polarizability with mole fraction of the binary system at different temperatures: ■, 293.15 K; ◆, 303.15 K; ▲, 313.15 K; ●, 323.15 K. The solid curves represent smoothed experimental data.

where N_A is Avogadro's number. The values of polarizability are calculated and given in Table 9 and Fig. 6, which show that the polarizability of the binary mixture is weakly affected by temperature and increases with the decrease of solvent. The polarizability of $[PiC_5Py][NTf_2]_2$ and ACN is 4.4001×10^{-30} m^3 and 5.6336×10^{-29} m^3 at 293.15 K, thereby indicating that the intermolecular dipole-dipole force instead of the dispersion force is dominant [45]. The dispersion force is induced by an instantaneous dipole and dominated by the molecular polarizability. The great ionic strength and polarizability generate a strong dispersion force. The polarizability depends on the total number of electrons and the volume over which they are spread. The polarizability values the increase with increasing concentration of $[PiC_5Py][NTf_2]_2$ in the binary mixtures.

CONCLUSIONS

Novel experimental data on the densities, dynamic viscosities and refractive indices of the pure IL $[PiC_5Py][NTf_2]_2$ and its binary mixtures with ACN at T of 293.15-323.15 K, as well as their entire composition range, were presented. From the experimental values, the volumetric properties of $[PiC_5Py][NTf_2]_2$ (1)+ACN (2) binary mixtures, and their V^E were obtained. The values of $\Delta\eta$ and ΔG^{*E} for the binary mixtures were calculated. The refractive indices, molar refraction, and polarizability were also induced. Negative deviations for the excess molar volumes, dynamic viscosities, and refractive indices were observed. The values of V^E, $\Delta\eta$ and Δn_D were fitted to the Redlich-Kister equation with satisfactory results. For the excess molar volumes, the strong ion-dipole interaction between the non-hydrogen bonding polar ACN and cations of $[PiC_5Py][NTf_2]_2$ dominated the volumetric property. The packing efficiency and temperature had a weaker influence on the binary mixture system. The modified VFT equation is an effective way to determine the fit of viscosity. The strong self-association of the solvent and the weak hydrogen bonding interaction between $[PiC_5Py][NTf_2]_2$ and ACN determine the $\Delta\eta$. The positive deviation of ΔG^{*E} for the binary mixtures illustrated that intermolecular hydrogen bonding interactions between $[PiC_5Py][NTf_2]_2$ and ACN are determinant; ΔH^* and ΔS^* of activation for the viscous flow similarly confirm this conclusion. The refractive deviation and polarizability can be explained by the dipole-dipole molecular interaction between $[PiC_5Py][NTf_2]_2$ and ACN.

ACKNOWLEDGEMENTS

This work was performed with the National Natural Science Foundation of China (No. 21176228), the Science and Technology Planning Project of Henan Province (No. 162102210056), the Foundation for University Key Teacher of Henan Province (No. 2013GGJS-108), and Science and Technology Research Projects of Zhengzhou City (No.141PQYJS555).

REFERENCES

1. A. Abo-Hamad, M. Hayyan, M. A. AlSaadi and M. A. Hashim, *Chem. Eng. J.*, **273**, 551 (2015).
2. H. Du, X. Lin, Z. Xu and D. Chu, *J. Mater. Sci.*, **50**, 5641 (2015).

3. M. Elnagdi, M. Moustafa, S. Al-Mousawi, R. Mekheimer and K. Sadek, *Mol. Divers.*, **19**, 625 (2015).
4. Y. Li, C. Zhang, Y. Zhou, Y. Dong and W. Chen, *Eur. Polym. J.*, **69**, 441 (2015).
5. D. R. MacFarlane, M. Forsyth, P. C. Howlett, J. M. Pringle, J. Sun, G. Annat, W. Neil and E. I. Izgorodina, *Acc. Chem. Res.*, **40**, 1165 (2007).
6. R. D. Rogers and K. R. Seddon, *Science*, **302**, 792 (2003).
7. J. E. Bara, T. K. Carlisle, C. J. Gabriel, D. Camper, A. Finotello, D. L. Gin and R. D. Noble, *Ind. Eng. Chem. Res.*, **48**, 2739 (2009).
8. M. Petkovic, K. R. Seddon, L. P. N. Rebelo and C. Silva Pereira, *Chem. Soc. Rev.*, **40**, 1383 (2011).
9. S. Zhang, J. Sun, X. Zhang, J. Xin, Q. Miao and J. Wang, *Chem. Soc. Rev.*, **43**, 7838 (2014).
10. X. Zhang, X. Zhang, H. Dong, Z. Zhao, S. Zhang and Y. Huang, *Energy Environ. Sci.*, **5**, 6668 (2012).
11. F. D'Anna and R. Noto, *Eur. J. Org. Chem.*, **2014**, 4201 (2014).
12. Z. Tang and S. Li, *Curr. Opin. Solid State Mater. Sci.*, **18**, 119 (2014).
13. J. L. Anderson and D. W. Armstrong, *Anal. Chem.*, **77**, 6453 (2005).
14. L. Zhang, H. Qi, Y. Wang, L. Yang, P. Yu and L. Mao, *Anal. Chem.*, **86**, 7280 (2014).
15. T. Hamamoto, M. Okai and S. Katsuta, *J. Phys. Chem. B*, **119**, 6317 (2015).
16. Z. Long, Y. Zhou, W. Ge, G. Chen, J. Xie, Q. Wang and J. Wang, *ChemPlusChem.*, **79**, 1590 (2014).
17. D. Wei-Li, J. Bi, L. Sheng-Lian, L. Xu-Biao, T. Xin-Man and A. Chak-Tong, *Catal. Today*, **233**, 92 (2014).
18. M. Atilhan, J. Jacquemin, D. Rooney, M. Khraisheh and S. Aparicio, *Ind. Eng. Chem. Res.*, **52**, 16774 (2013).
19. I. Bahadur, T. M. Letcher, S. Singh, G. G. Redhi, P. Venkatesu and D. Ramjugernath, *J. Chem. Thermodyn.*, **82**, 34 (2015).
20. F. Nabi, M. Malik, C. Jesudason and S. Al-Thabaiti, *Korean J. Chem. Eng.*, **31**, 1505 (2014).
21. M. Sattari, A. Kamari, A. H. Mohammadi and D. Ramjugernath, *J. Taiwan Inst. Chem. E.*, **52**, 165 (2015).
22. X. Zhang, F. Huo, X. Liu, K. Dong, H. He, X. Yao and S. Zhang, *Ind. Eng. Chem. Res.*, **54**, 3505 (2015).
23. R. Majdan-Cegincara, M. T. Zafarani-Moattar and H. Shekaari, *J. Mol. Liq.*, **203**, 198 (2015).
24. F. Chen, Z. Yang, Z. Chen, J. Hu, C. Chen and J. Cai, *J. Mol. Liq.*, **209**, 683 (2015).
25. M. S. Rahman, M.A . Saleh, F. I. Chowdhury, M. S. Ahmed, M. M. H. Rocky and S. Akhtar, *J. Mol. Liq.*, **190**, 208 (2014).
26. M. Geppert-Rybczyńska, A. Heintz, J. K. Lehmann and A. Golus, *J. Chem. Eng. Data*, **55**, 4114 (2010).
27. H.-C. Ku and C.-H. Tu, *J. Chem. Eng. Data*, **43**, 465 (1998).
28. A. K. Nain, S. Ansari and A. Ali, *J. Solution Chem.*, **43**, 1032 (2014).
29. R. K. Shukla, A. Kumar, N. Awasthi, U. Srivastava and V. S. Gangwar, *Exp. Therm. Fluid Sci.*, **37**, 1 (2012).
30. J. Chen, L. Chen and Y. Xu, *J. Chem. Thermodyn.*, **88**, 110 (2015).
31. A. Zhu, J. Wang and R. Liu, *J. Chem. Thermodyn.*, **43**, 796 (2011).
32. M. Geppert-Rybczyńska, J. K. Lehmann and A. Heintz, *J. Chem. Thermodyn.*, **71**, 171 (2014).
33. M. Geppert-Rybczyńska and M. Sitarek, *J. Chem. Eng. Data*, **59**, 1213 (2014).
34. J.-Y. Wu, Y.-P. Chen and C.-S. Su, *J. Solution Chem.*, **44**, 395 (2015).
35. M. Anouti, A. Vigeant, J. Jacquemin, C. Brigouleix and D. Lemordant, *J. Chem. Thermodyn.*, **42**, 834 (2010).
36. E. Gómez, N. Calvar, Á. Domínguez and E. A. Macedo, *J. Chem. Thermodyn.*, **42**, 1324 (2010).
37. M. Anouti, J. Jacquemin and D. Lemordant, *J. Chem. Eng. Data*, **55**, 5719 (2010).
38. T. Zhao, J. Zhang, L. Li, B. Guo, L. Gao and X. Wei, *J. Mol. Liq.*, **198**, 21 (2014).
39. A. Pal and A. Kumar, *Fluid Phase Equilib.*, **143**, 241 (1998).
40. T. Zhao, J. Zhang, B. Guo, F. Zhang, F. Sha, X. Xie and X. Wei, *J. Mol. Liq.*, **207**, 315 (2015).
41. I. Banik and M. N. Roy, *J. Chem. Thermodyn.*, **63**, 52 (2013).
42. L. F. Sanz, J. A. González, I. García De La Fuente and J. C. Cobos, *J. Mol. Liq.*, **172**, 26 (2012).
43. A. Chełkowski, Dielectric physics, Elsevier Science & Technology (1980).
44. H. Shekaari, M. T. Zafarani-Moattar and S. N. Mirheydari, *J. Chem. Eng. Data*, **60**, 1572 (2015).
45. G. R. Sunkara, M. M. Tadavarthi, V. K. Tadekoru, S. K. Tadikonda and S. R. Bezawada, *J. Chem. Eng. Data*, **60**, 886 (2015).
46. P. Diaz-Rodriguez, J. C. Cancilla, N. V. Plechkova, G. Matute, K. R. Seddon and J. S. Torrecilla, *Phys. Chem. Chem. Phys.*, **16**, 128 (2014).
47. Y. Kayama, T. Ichikawa and H. Ohno, *Chem. Commun.*, **50**, 14790 (2014).